Journal of Vibration Engineering & Technologies
https://doi.org/10.1007/s42417-024-01512-y

ORIGINAL PAPER

Investigation of Transverse Cracks with Different Orientations in GFRP Beam Through Modal Data Based ANN Model

Pankaj Chaupal[1] · **Prakash Rajendran**[1]

Received: 1 February 2024 / Revised: 6 July 2024 / Accepted: 9 July 2024

Abstract

Purpose Glass fiber reinforced polymer (GFRP) composite structures are extensively utilized across the globe due to their lightweight, corrosion resistance, high specific strength and stiffness. Generally, fatigue failures are common in composite structures such as aircraft structures, mechanical components, windmill structures, etc. The crack initiates and propagates in relative orientation between the crack and loading direction which adversely affects the performance of composite structures. Therefore, it is essential to detect the crack location and orientation to avoid catastrophic failure. This research article explores the investigation of transverse cracks with different orientations in GFRP composite beams using a modal data-based Artificial Neural Network (ANN).

Methods The composite beam laminate is fabricated using vacuum-assisted resin transfer molding with bi-directional GFRP lamina. Crack with consistent depth and triangular shape made on the specimen using a hacksaw. Experimental modal analysis is carried out on four beam specimens with different damage conditions such as without crack and transverse crack with 30, 60, and 90-degree orientations under cantilever boundary conditions. Further, ANN is applied to the modal parameters to predict the frequency response functions (FRFs).

Results To comprehend the specimen's behavior for notable changes, modal parameters such as natural frequencies, mode shapes, damping ratios and FRFs are acquired and briefly examined for various experimental cases. Then, FRFs for all four cases are predicted using ANN, and the accuracy of the model is computed.

Conclusion It is observed that for the fundamental mode, natural frequencies decrease and damping ratios increase respectively with the formation of crack. The predicted FRFs using ANN have agreed well with the experimental FRFs for all different criterion.

Keywords GFRP · Beam structure · Transverse crack · Crack orientation · Modal analysis · ANN model

Introduction

Significant progress has been made in the development of fiber-reinforced polymer composite over several decades due to superior physical, chemical, and mechanical characteristics [1, 2]. These materials anticipate several mechanical advantages, such as design simplicity, safety, and service life. They have acquired prominence in a variety of disciplines because of their high stiffness to weight ratio, high strength to weight ratio, and low production cost. These contemporary materials are primarily used across a wide range of industrial fields, including aerospace, automotive, construction and transportation [3–6]. In aeronautical, civil and mechanical systems damages are inevitable. The structural integrity and load-bearing capability of a GFRP beam design may be jeopardized by a crack. It develops due to fatigue, manufacturing flaws and when the stresses at the fracture tip surpass the allowable limit [7, 8]. The sustained actions of the structural element are threatened by cracks. Safety and preventive measures should be a top priority to maintain the structural integrity [9]. These days, monitoring the health of structures is crucial. The methods for local and global damage analyses are frequently employed for crack identification and to maintain structural integrity [10–13].

Global-based damage identification method identifies damage based on changes in vibrational characteristics viz natural frequencies, mode shapes and damping ratios [14].

✉ Prakash Rajendran
rprakash@nitt.edu

[1] Department of Mechanical Engineering, National Institute of Technology, Tiruchirappalli, Tamil Nadu 620015, India

Published online: 19 July 2024

When analyzing the FRF curves, the resonance frequency's peak is used to determine the natural frequencies [15, 16]. Khalate & Bhagwat [17] explored that the crack present near the fixed end of the cantilever beam has a significant decrease in natural frequency as compared to the free end with the same length and depth of the crack. Additionally, they concluded that as crack depth increases, the natural frequency drastically decreases. Das & Yilmaz [7] investigated transverse open crack on a curve composite beam experimentally and numerically. They found that altering the position and depth of the cracks did not always cause the natural frequency to decrease. This behavior of the structures might be concerned with the closeness of the crack to the fixed and free end node positions. Jena et al. [18] examine the dynamic behavior of cracked composite beams by varying the angle of the bidirectional fiber. They observed that the relative natural frequency of the beam decreases with relative crack depth, relative crack length and fiber orientation from 0^o to 45^o due to stiffness degradation. The maximum frequency is observed corresponding to 0^o fiber orientation. Mehdi et al. [19] estimated that the frequency of the structures decreases drastically as the number of cracks on the beam increases. Many investigations observed that when the crack is situated distant from the fixed end, the frequency shift is insignificant as compared to the free end [20, 21]. It is also observed that damage severity increases with increasing depth of crack because of stiffness reduction [4, 22]. Natural frequency-based damage detection systems are less sensitive and unreliable in finding little and precise damages [12]. As a result, integrated natural frequency and mode shape-based approaches are employed to overcome the shortcomings [23].

Kahya et al. [24] identified the presence and location of multiple cracks in a fixed-free beam using natural frequencies and mod shapes. Doninski & Krawczuk [25] computed mode shapes of undamaged and intact wind turbine blades employing numerical and experimental modal analysis and predicted the presence and location of damage. Mode shape-based method can only locate the presence of damage and can't ensure the damage severity. Hence, Gorgin [26] applied the damage index method based on the first mode shape on a beam structure to predict the size and severity of the damage. Mode shape data-based indicator used by Yazdanpanah et al. [27] for damage detection in a beam structure, and it was summarized that the suggested approach was more effective than the curvature damage factor. To locate the damage in a GFRP composite beam structure, Rajendran & Srinivasan [28] employed the modal-based damage parameters such as force index and rotational curvature index computed using experimental mode shape data. Further damping ratios also come into pixels to identify significant damage in composite structures. In a composite cantilever beam, Demir [29] investigated the natural frequencies and damping ratios and found that they decrease as hole diameter increases. Kiral et al. [30] found that damping ratios increase with increasing damage severity, and it is more sensitive at the clamped edge. The damping ratio is highly susceptible to beam failures as compared to the natural frequency. The position and intensity of the failures also significantly impact the damping ratios. Kyriazoglou et al. [31] found that vibration damping increases substantially prior to the fatigue failure.

Vibration-based methods (VBMs) are not reliable for solving major structural damage problems alone. Thus, VBMs are combined with signal processing and artificial intelligence techniques for solving advanced structural damage problems. Rajendran & Srinivasan [32] applied wavelet packet transform as a signal processing technique to identify damage in a plate structure in the form of added mass. Rajendran & Sivakumar [33] used rotational mode shape as a parameter in the wavelet packet transform (WPT) to detect damage in a glass fiber beam structure. ANN technique is presently a very successful technique in automated structural health monitoring. Chaupal & Rajendran [34] utilized the ANN model to estimate the flexural strength of randomly oriented chopped GFRP composite laminate using three-point bending test data. Using ANN model and vibration parameters, Tan et al. [35] located and quantified damage in a girder-bridge composite slab. Jena et al. [36] applied first three modes natural frequencies and fiber orientation as input to the neural network technique and predicted relative crack length and depth in an FRP beam. Sahoo & Jena [11] applied crack length and crack depth as input parameters to the ANN and predicted the first three natural frequencies of the beam. It was shown that the relative natural frequency increases with increasing relative crack length and reduces proportionately with increasing relative crack depth. Zara et al. [3] fed natural frequency as an input and predicted the exact crack length as an output using improved ANN using different optimization algorithms. Mojtahedi et al. [37] tested random decrement signature methods and the ANN algorithm to identify the damage (increased mass). They provided natural frequency, mode shape, and damping ratio as input to the ANN model. It reveals that when there is damage, the coherence function decreases. Zhang et al. [38] employed ANN model and surrogate-assisted genetic algorithm to determine the position, size, and interface of delamination in a CFRP curved plate composite. The algorithm demonstrates how the backpropagation ANNs approach uses frequency shifts as input parameters and the location and size of interface delamination as output parameters. Oliver et al. [39] applied ANN based on frequency variation and determined the location and extent of delamination damage in a composite plate construction. Reis et al. [40] used ANN based on FRF to identify different sizes of delamination

in a GFRP beam. Sreekant et al. [41] detected the location and size of delamination in a composite beam using ANN based on vibration response. Sreekant et al. [42] determined the position and location of delamination in a GFRP composite plate using ANN by applying the change in natural frequencies as an input parameter.

According to a summary of previous research, numerous studies have been conducted to predict the existence, location, and severity of cracks and delamination damages in a composite structure using ANN in conjunction with variations in natural frequencies, mode shapes, and damping ratios. However, limited work has been carried out on the vibration analysis of a GFRP composite beam laminate with traverse open crack with varying orientations in concurrence with the application of the ANN model. Therefore, the novelty of this research work is to investigate transverse cracks with various orientations in GFRP composite beams using ANN based on vibrational characteristics. In this research work, four glass fiber composite beams are fabricated using vacuum-assisted resin transfer molding. After fabrication, a triangular crack of constant depth is created in the middle with 0, 30, 45 and 60-degree crack orientation. Further, experimental modal analysis were performed on the beam under cantilever boundary conditions. Thereafter, vibrational characteristics are analyzed, and ANN is applied to predict the FRF. This research article is arranged as follows: The materials and methodology are described in sect. 2. The materials and methodology include the fabrication of composite using vacuum assisted resin transfer molding, experimental modal analysis and the method of ANN simulation. Section 3 provides a brief presentation of the findings and comments, along with vibration characteristics, FRFs and outcomes that were anticipated using ANN. Finally, the concluding remarks are presented in sect. 4.

Materials & Methods

Fabrication

The composite laminates such as beam, plate and shell can be fabricated using hand lay-up process, resin transfer molding and vacuum extrusion process. In this study, the GFRP beam is manufactured through Vacuum Assisted Resin Transfer Moulding (VARTM) and followed by cutting process. It begins with cleaning of the mould using wax which is followed by the application of polyvinyl alcohol. Polyvinyl alcohol acts as a releasing agent that allows the GFRP laminate to be readily removed from the mould surface after curing. A suitable size of 200 gs per square meter (GSM) GFRP lamina is cut with scissors and placed over the mould surface one by one, up to the specified thickness in a suitable fibre orientation. An appropriate size of peel ply and infusion mesh is cut and positioned above the lamina. The spiral tube and vacuum connector are placed above the infusion mesh at the input, and the output ends are secured using masking tape. Then, the entire assembly is kept inside the vacuum bag, which is prepared using the heat-sealing machine and sealing tape. Finally, a hose pipe is linked to the connector's input and outlet end and placed into the resin holder and resin catch pot respectively. Each inlet and outlet end of the resin fusion line has one resin fusion line clamp to check the resin flow. The catch pot hose is attached to the vacuum pump and securely sealed with masking tape, and the pump is turned on, which removes all the air from the vacuum bag and displays a negative pressure on the pressure gauge.

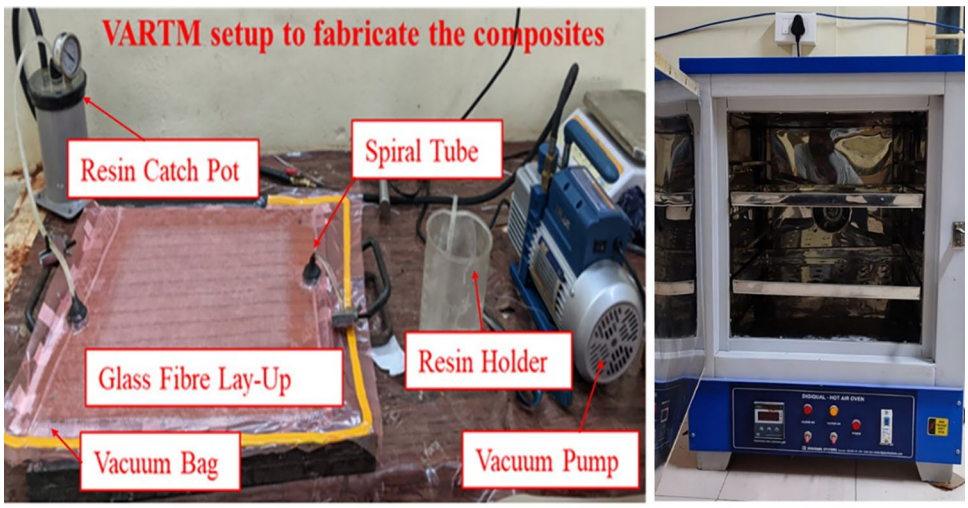

Fig. 1 Schematic representation of **a** VARTM setup and **b** hot air oven

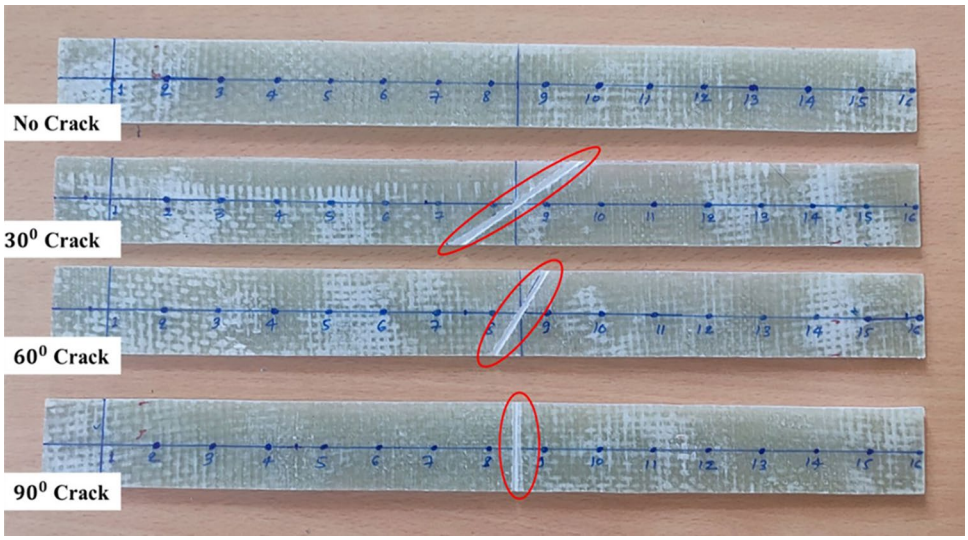

Fig. 2 GFRP beam with no crack, 30°, 60°, and 90° crack orientation

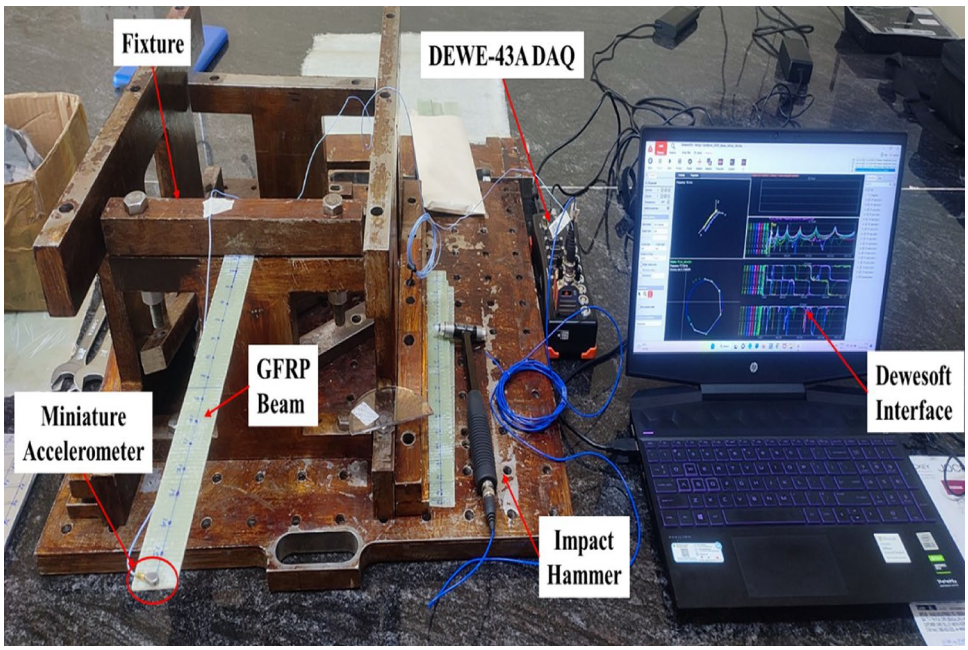

Fig. 3 Schematic representation of experimental modal analysis setup

In a separate beaker, the fibre to epoxy ratio is considered as 1:1 equally by weight and epoxy to hardener is taken as 10:1 by weight [43, 44] are mixed together. Using a magnetic stirrer, they are well blended. In the vacuum bagging configuration, two pipe connections are set up: one pipe is dipped into the beaker, and another pipe is linked to the vacuum pump via the resin catch pot as shown in Fig. 1(a). The first resin input pipe is closed, and all air is pulled out which results in a negative pressure in the gauge. Check for any leakage in the bagging before allowing epoxy and hardener to flow through the stacked lamina. Allow the mixture to flow until the whole lamina has been filled with the epoxy and hardener mixture. After that, shut the input line and let the vacuum pump remove any remaining matrix material. Close the outlet and turn off the entire system after reaching the proper proportion. Remove the excess pipe while keeping the pipe's inlet and outlet closed. The entire arrangement was then placed in a hot oven with the temperature set to 60 °C for 24 h to cure as depicted in Fig. 1(b). Once the material has been set, remove it from the bag, remove any undesired particles. At last, the laminate is cut into a beam shape of dimensions 300 mm * 30 mm * 2 mm, and a triangular crack of depth of 1 mm is made above the beam in the middle with an orientation of 30°, 60° and 90° respectively using hacksaw blade as shown in Fig. 2.

Experimental Modal Analysis

The experimental modal analysis (EMA) was performed on the four GFRP specimens with different crack orientations. Mostly, the cantilever type beams are used in aircraft structures. Thus, the prepared GFRP specimen is setup in the fixture as a cantilever type beam as shown in Fig. 3. The beam is discretized into fifteen parts with each 20 mm apart. The miniature accelerometer (Model: PCB 352A21 & Sensitivity: 10 mV/g) is mounted on the free end with the help of glue. The other end of miniature accelerometer BNC cable is connected to the DEWE 43A DAQ (8 channels USB data acquisition system). Further, impact hammer (Model: 086C01 & Sensitivity: 11.2 mV/N) is also connected to the DAQ. The DEWE 43A DAQ is connected to the PC with the DEWESOFT-X-EDU Software interface. Further, In the DEWESOFT-X-EDU Software, necessary parameters such as resolution, sensitivity, excitation, response, geometry, etc., were defined, and the roving hammer method was chosen for the modal analysis. Once the modal analysis is performed the necessary data is imported into the excel format like FRF, acceleration response, impact force response, mode shape and damping ratio. Further, the investigation is completed on these imported datasets to predict the damage locations and orientations for different cases.

Artificial Neural Network Simulation

The process of implementing ANNs to forecast the frequency response function of GFRP composite laminates is shown in Fig. 4. To determine the model input (amplitude) and output (natural frequency) parameters, free vibration analysis was first carried out using an experimental modal analysis (EMA) setup. For this ANN simulation, the ANN design with 16 input layers, 70 hidden layers, and 1 output layer is used. In total, 7814 (length of FRF) data points were obtained from the modal test and analyzed. Additionally, the data points are split into 70:15:15 proportions for testing, validation, and training, respectively. The sigmoid and purelin functions were used on the hidden and output layers, respectively. The architecture of ANN model is simulated in MATLAB®2021a to train, validate and test the ANN model. The computer workstation has a 2.50 GHz Intel(R) Core (TM) i5-10300 H CPU and 8 GB of RAM. The L-M approach is used to train the ANN model, and the number of neurons in the hidden layer is optimized for the lowest RMS error values. Following that, the model's performance, error histogram, and regression are thoroughly examined to determine the model's correctness. Finally, the FRF is predicted and compared to the experimental findings to assess the ANN model's efficacy and dependability.

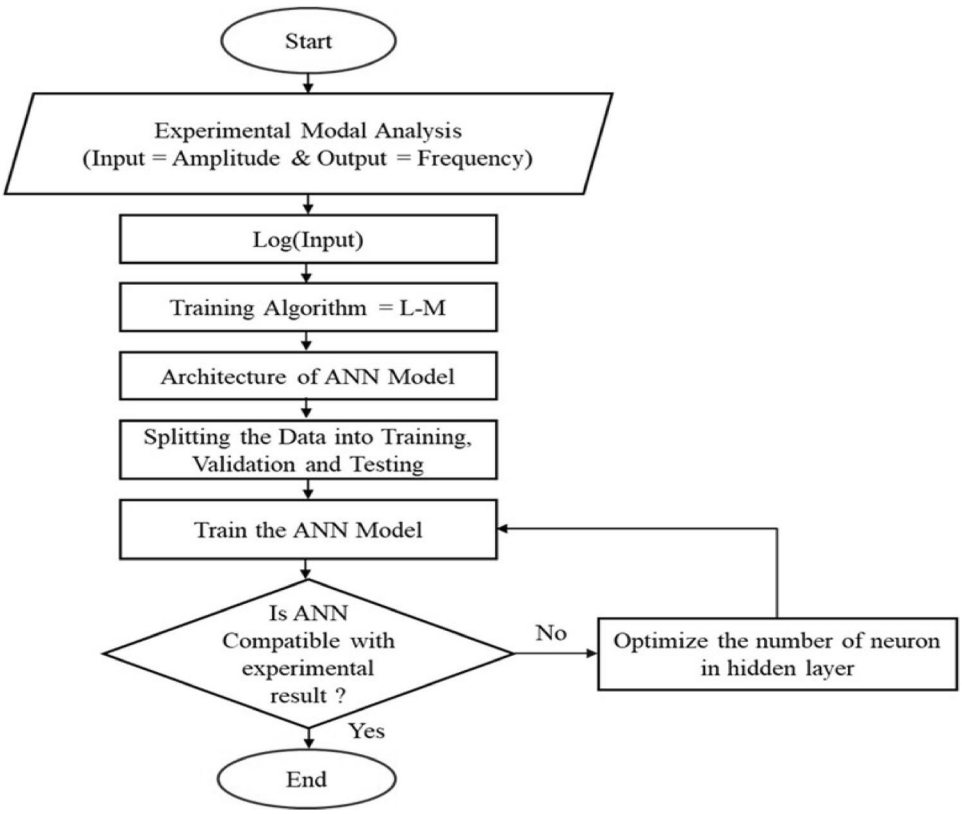

Fig. 4 Artificial neural network methodology

Results and Discussions

The EMA and ANN simulation results of the GFRP beam under cantilever boundary conditions are briefly explained in this section. After experimental modal analysis of FRF, natural frequencies, mode shape and damping ratios are investigated and the effect of different crack orientations on these vibrational characteristics are studied. Based on the obtained vibration parameters, ANN models were developed to predict the FRFs of the GFRP composite beam.

Vibration Characteristics

Figure 5 shows the schematic of DEWESOFT-X-EDU interface after the experimental modal analysis using roving hammer method. The representation of natural frequency, damping ratio, mode shape, FRF, phase angle and coherence can be clearly observed in the Dewesoft interface.

Frequency Response Function

The FRFs of GFRP beams are extracted from experimental modal analysis as given in section 2.2. Representation of experimental FRF curves for beams with different cases such as without crack, crack orientations 30 °, 60 ° and 90 ° are clearly shown in Fig. 6. It is clearly observed that there is shift in FRF curves with formation of crack. The first and second mode shapes are more dominant and shift in FRF results in decrease in natural frequencies as compared to the intact beam. However, there is no trend observed in higher modes between intact and crack specimens.

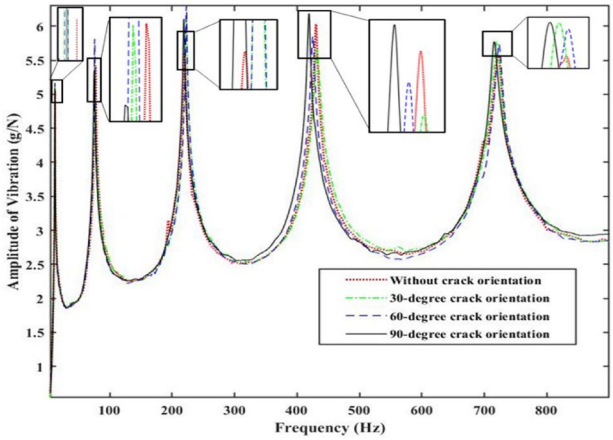

Fig. 6 Frequency response function of a beam under different crack orientations

Natural Frequencies and Damping Ratios

The experimental natural frequencies and damping ratios for different modes with varying crack orientations are given in Table 1. It is observed that the first and second modes, the natural frequency of the crack beam decreases as compared to the intact beam irrespective of the crack orientation. Hence, it is difficult to conclude the judgment based on the higher modes of natural frequencies.

The damping ratio is a type of damage signature can also vary based on the crack's location, orientation, and

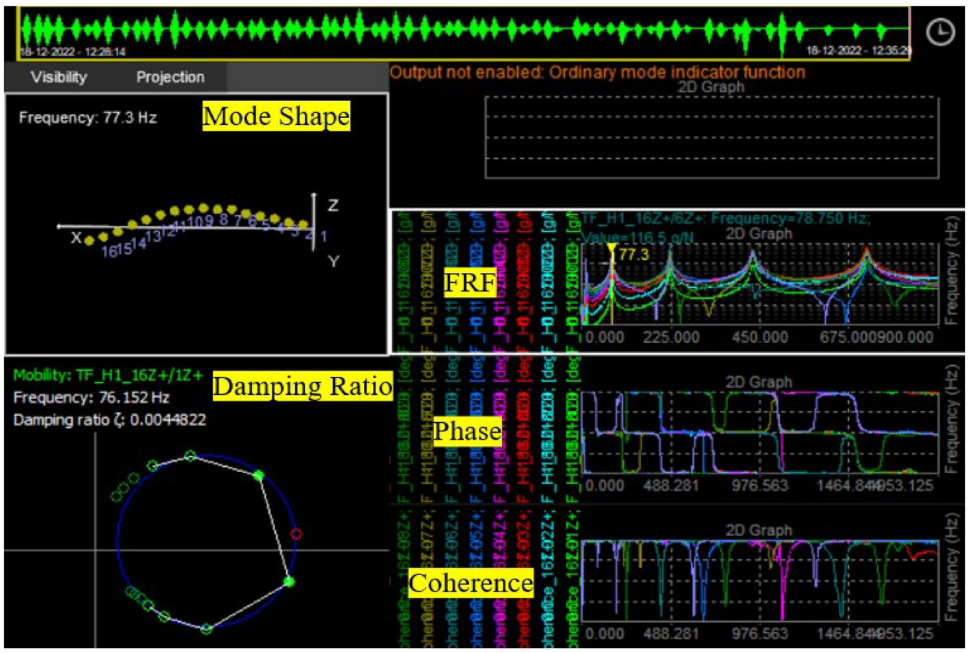

Fig. 5 Schematic of DEWESOFT-X-EDU interface

Table 1 Natural frequencies and damping ratios of the beam with varying crack parameters for different modes

Types of orientation	Mode 1		Mode 2		Mode 3		Mode 4		Mode 5	
	$\omega_n(Hz)$	$\xi(\%)$	$\omega_n(Hz)$	$\xi(\%)$	$\omega_n(Hz)$	$\xi(\%)$	$\omega_n(Hz)$	$\xi(\%)$	$\omega_n(Hz)$	$\xi(\%)$
No Crack	12.42	0.21	77.71	0.62	220.32	0.8	430.63	0.42	722.63	0.54
30°- Crack	12.2	1.08	76.15	0.44	222.79	0.38	431.83	0.71	719.31	0.65
60°- Crack	12.23	1.04	76.13	0.49	222.73	0.36	425.25	0.49	723.13	0.53
90°- Crack	12.34	1.02	75.35	1.48	218.82	0.41	418.98	0.4	715.85	0.6

severity. The damping ratio of first mode is observed increases for different crack orientation cases with respect to intact beam. The increase in damping may be due to energy dissipation in the crack region. Further, the trend of damping ratio decreases relatively as crack orientation increases. However, it is challenging to predict the trend in the higher modes.

Mode Shapes

In this section, the first five experimental modes of the GFRP beam under clamped-free boundary conditions are explained for four different cases of the beam. In the Figs. 7 and 8 , the x-axis represents the nodal point distance from the fixed end of the beam and z-axis shows displacement of each nodal point. It is observed that there is no evidence found in mode shapes. The higher mode shapes of cracked beams with orientation of 30°, 60° and 90° show insignificant changes as shown in Figs. 7 and 8. The sign of crack is not clearly seen with the mode shapes of beams. With only modal parameters, it is arduous to detect the crack location and orientation. Thus, it is suggested to use FRF curves of beams in ANN models to predict the crack location and orientation accurately in the beam.

Prediction of Frequency Response Function

Architecture of ANN Model

The architecture of multilayer perception or ANN is shown in Fig. 9. The ANN architecture selection is purely based on analyzing the partial derivative of the model's output relative to the model's input [45]. sixteen input layers, one output, and one hidden layer are selected for the simulation. Sigmoid and purlin functions were used in the hidden and output layers. Weight and biases are represented by W and b, respectively. The number of hidden layers is selected based on empirical justification. For linear problems, generally, one hidden layer is good enough, and for non-linear

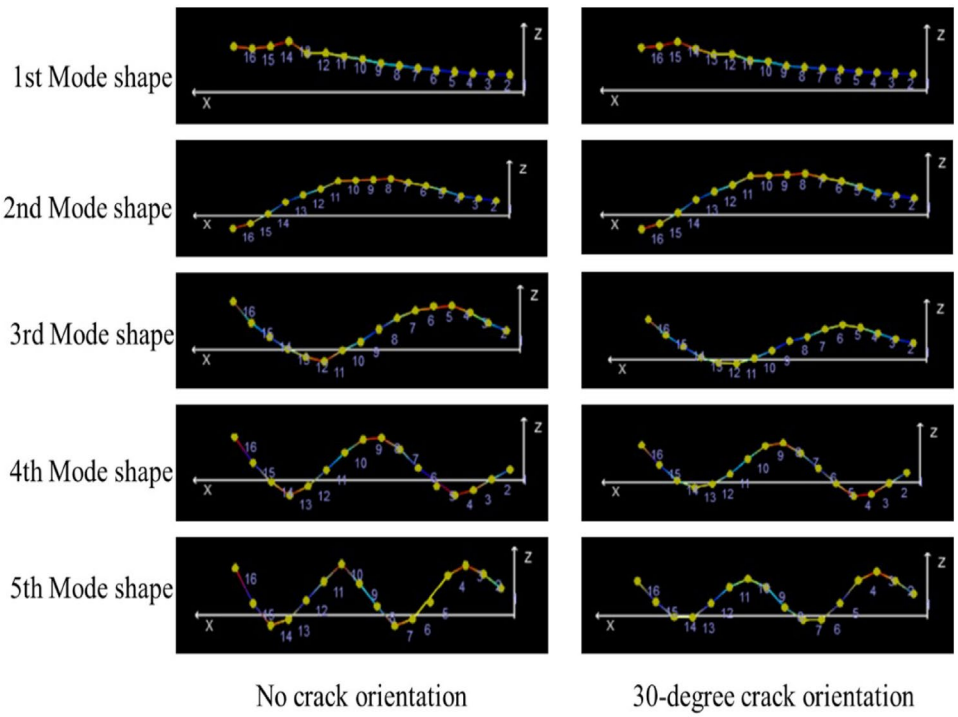

Fig. 7 Mode shape representation of the beam with no crack and 30° crack orientations

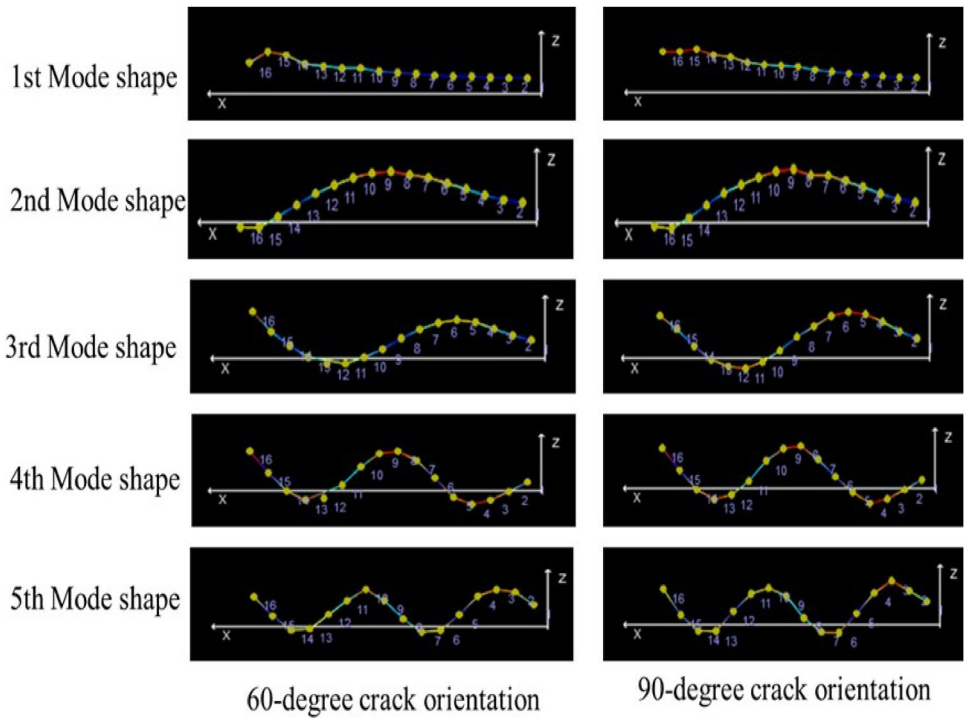

Fig. 8 Mode shape representation of the beam with 60° and 90° crack orientations

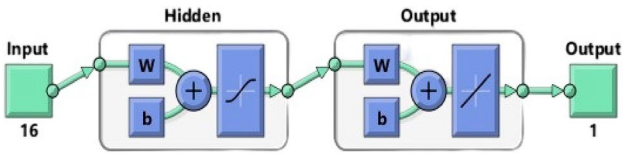

Fig. 9 Architecture of ANN

problems, more than one hidden layer is selected in ANN [34]. Further, the number of neurons in the hidden layer is optimized using hidden layer optimization techniques.

Hidden Layer Optimization

Optimizing the number of neurons in an ANN's hidden layer is critical to creating an effective neural network architecture. The hidden layer in the ANN model is the layer between the input and output layers. The appropriate number of neurons in the hidden layer can be determined by a variety of parameters and frequent experimentation. The computation functions employed in the hidden layer are used to resolve nonlinear problems. Therefore, determining the total number of hidden layers and the number of neurons in each hidden layer is essential. One cannot be assured of the number of concealed layers directly. Thus, it was computed by trial and error method. Zero hidden layers are often utilized for linear issues, while one or more hidden layers are used for complex problems. For this ANN study, just one hidden layer was selected. By computing a plot between the number of neurons and root mean square (RMS), as shown in Fig. 10. It is observed that corresponding to the 70 neurons in the hidden layer, the RMS values for the training, validation, and testing are minimal. Hence, number 70 is selected as an optimum number of neurons in the hidden layer for the further proceedings ANN simulations.

Parameters of ANN Model

Figure 11a–c represents the training state, performance and error histogram of the ANN model. These diagrams are the case with no crack condition of the beam. The training process of the current model is completed at nineteen epochs, as shown in Fig. 11a and b, but it does not give the minimum mean square error. Thus, the algorithm selects thirteen as the optimum number of epochs, corresponding to the most negligible MSE value. At this point, testing and validation errors remain constant, and test error decreases. Corresponding to the thirteen epochs a good fit is achieved, i.e., the ANN model is neither underfit nor overfit.

From Table 2, it is observed that the structure of the ANN model is chosen the same for all cases of the beam. There were sixteen input parameters, one output parameters and one hidden layer with 70 neurons. The simulation time for all the models is quite low i.e., less than 10 sec. Totally, 1000 epochs or iterations were defined for simulating the model, but the model can complete the computation within a smaller number of epochs i.e., approximately 25 epochs. The performance represents the highest accuracy and lowest

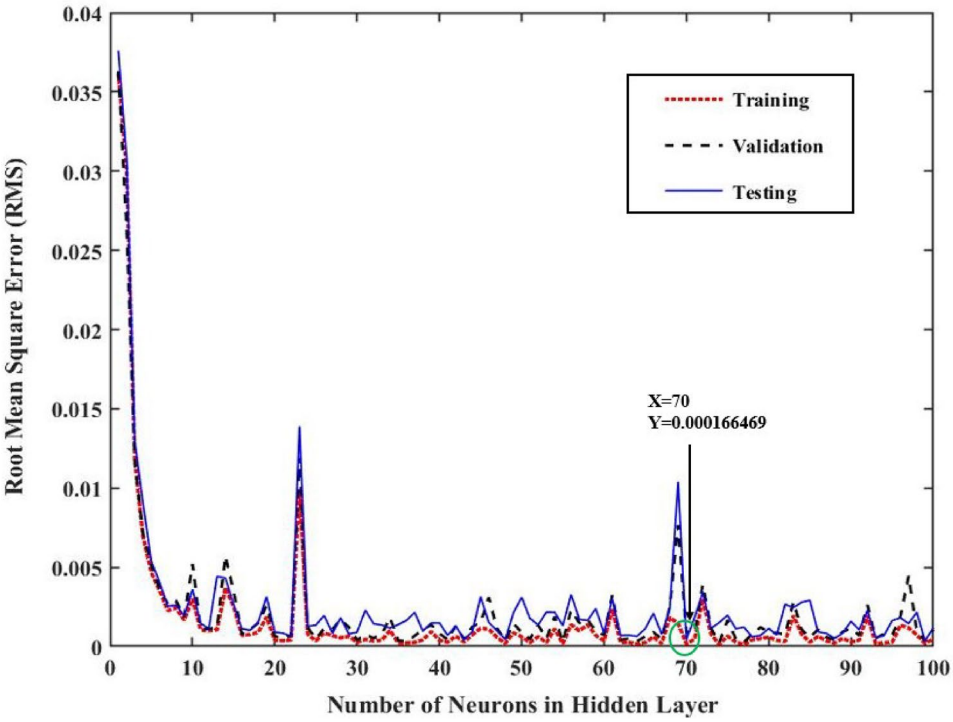

Fig. 10 Optimization of the number of neurons in a hidden layer

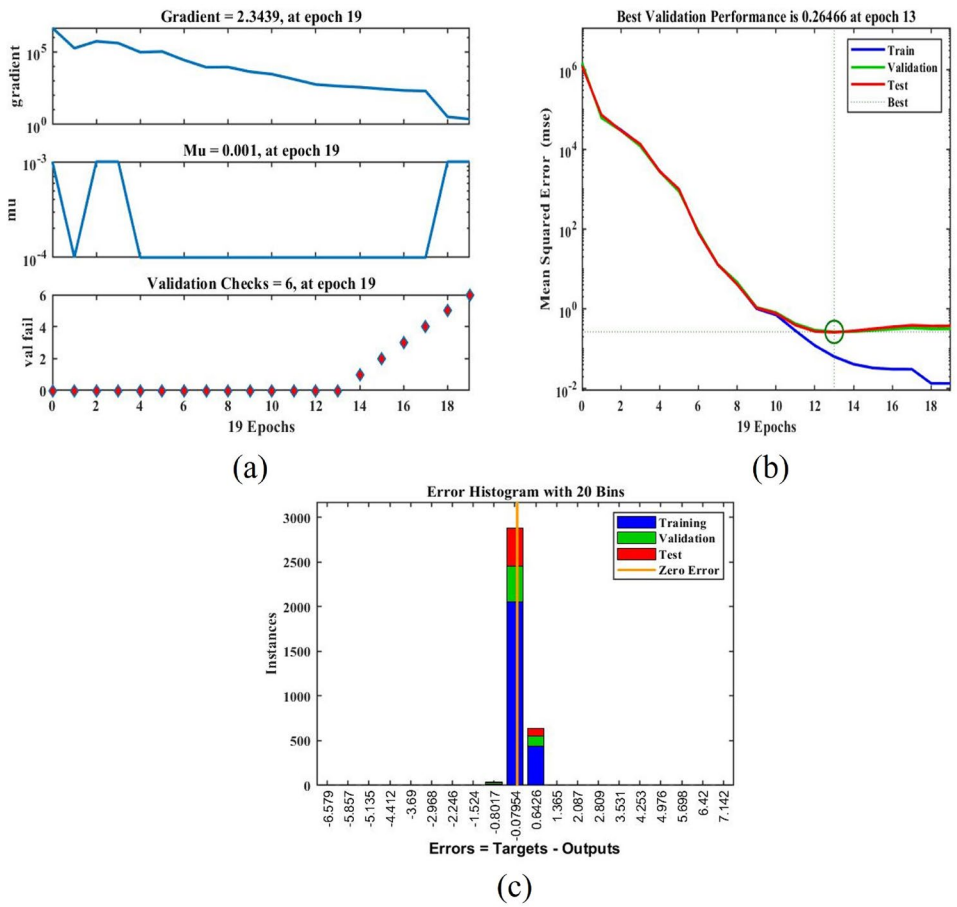

Fig. 11 **a** Training state of the model, **b** Performance of the model, **c** Error histogram

Table 2 Parameters of artificial neural network (ANN) simulation

Types of crack	Network structure	Time (Sec)	Epoch	Performance	Gradient	Mu	Error histogram	RSME(%)		
								Train	Val	Test
No-Crack	16-70-1	6	19	0.0231	225	0.0001	− 3.348 to 2.21	0.2207	0.3496	0.3404
30°-Crack	16-70-1	7	24	0.321	330	0.001	− 3.11 to 0.9576	0.1942	0.333	0.2747
60°-Crack	16-70-1	10	23	0.0121	76.3	0.0001	− 4.206 to 3.444	0.2126	0.3183	0.43
90°-crack	16-70-1	6	19	0.0136	2.34	0.001	− 6.579 to 7.142	0.2523	0.5144	0.5087

loss on the validation data set. The performance value is the mean square error of the epoch size minus six. It is also called the best validation performance, in which training, validation, and testing have the least mean square error. The gradient represents the slope or rate of change of the loss function with respect to the network's parameters. It guides the parameter updates during training to minimize the loss, thereby improving the network's ability to make accurate predictions.The learning rate is represented by Mu and it is a crucial hyper-parameter in training ANN models using optimization algorithms like gradient descent, stochastic gradient descent (SGD), Adam, RMSprop, L-M, and others. It determines the step size at which the model's weights are updated during the training process. The present model is trained by L-M training algorithm. An error histogram shows the graphical representation of the distribution of prediction errors made by the network on a dataset. It helps us to visualize how well our neural network is performing and provides insights into the nature of prediction errors. A twenty-bin system was used for the analysis. It is observed that the majority of datasets are close to the zero line. Hence, the trained model can predict the future successfully. The RMSE values for all cases of damages are less than 1%. Hence, the parameters listed in the above table are efficient and can efficiently predict future datasets.

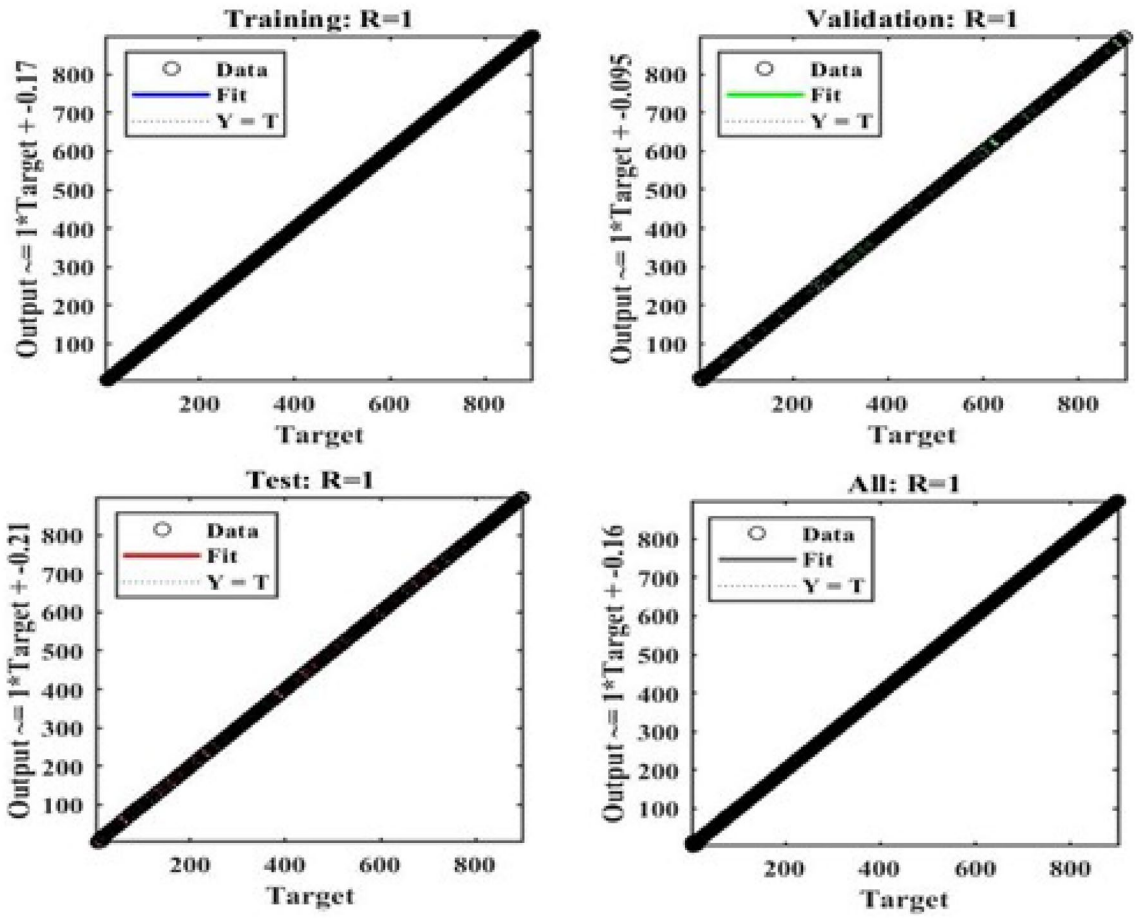

Fig. 12 Regression values for **a** Training, **b** Validation, **c** Test and **d** Combined results

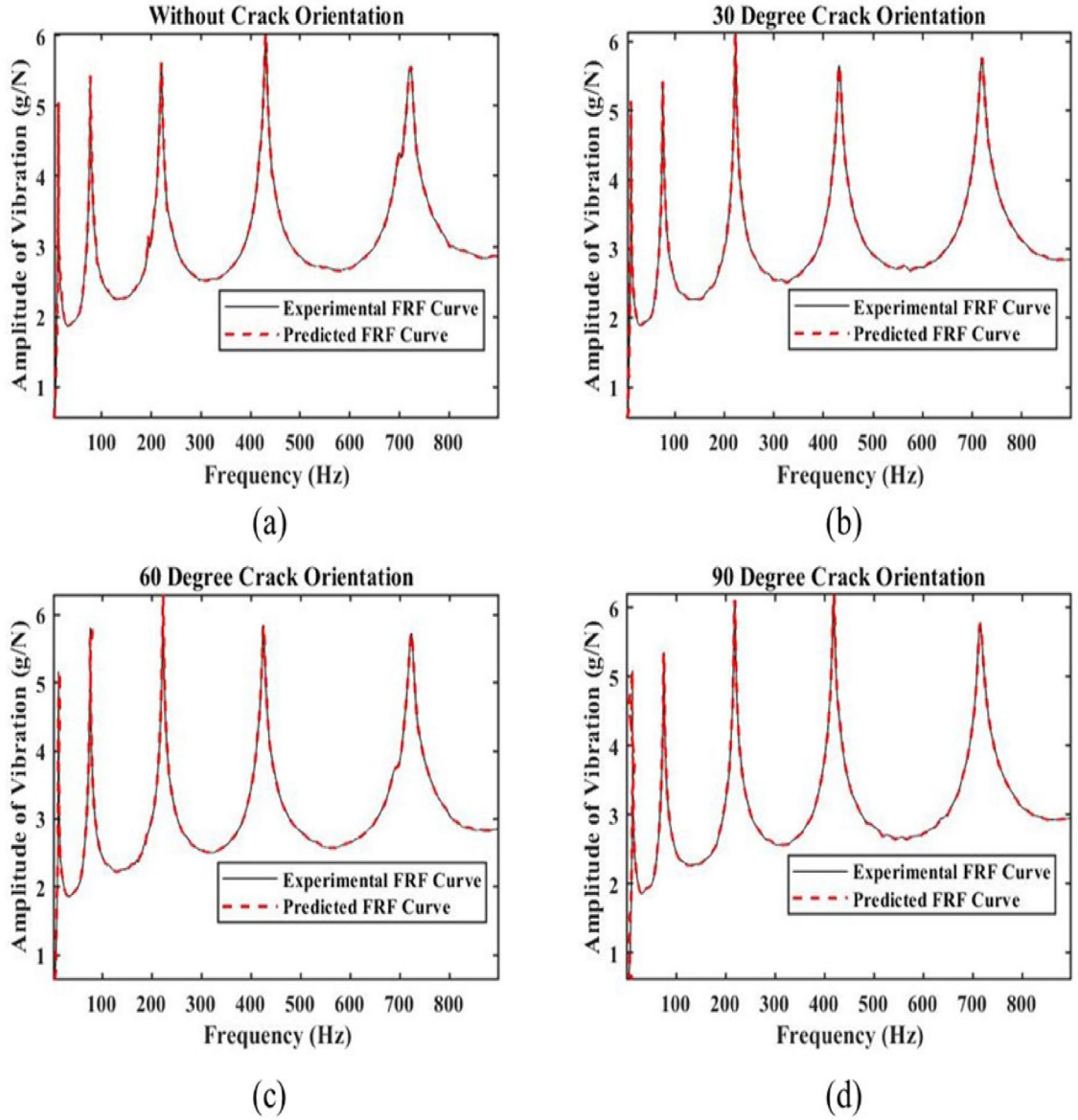

Fig. 13 Comparison between experimental and predicted FRF curves

Regression Value

The ANN models' regression values generated for training, validation, and testing are 1, as shown in Fig. 12a–c. However, the overall regression value of 1 for testing, validation, and training as shown in Fig. 12d. The data sets for the test, validation, and training components are fitted along the regression line. It revealed a strong relationship between the analysis and the desired results.

Predicted FRF Curves

The experimental and predicted FRF curves of a GFRP beam with all four scenarios of crack i.e., beam without crack, with 30^0, 60^0, and 90^0 crack orientations are shown in Fig. 13. It is observed that predicted FRF curves for all cases of cracks have good agreement with the experimental FRF curves. The RMSE for training, validation and test are less than 1% as shown in Table 2. Hence, it is justified that the present ANN model is highly efficient and can accurately predict the FRFs of the GFRP composite beam.

Conclusions

Crack has a noteworthy effect on the integrity of the structural components. The presence of the crack in the structure not only degrades the mechanical and dynamic properties of structures also it causes a catastrophic failure of structures. The existence of transverse crack on the structure cause adverse effects on modal characteristics viz degrade in natural frequency, altering the mode shapes and increase in damping ratio usually. If the nature of transverse crack changes i.e., crack is rotated with different angles. There might be detrimental effects on the dynamic properties of the structure. The observation of this study is as follows: (i) for 90^0 crack orientation, the natural frequency of beam decreases for all modes as compared to intact beam. (ii) it is observed that the natural frequency may increase or decrease for higher modes (other than 1^{st} & 2^{nd}) if the orientation of open transverse crack is not perpendicular to the axis of the beam. (iii) For the fundamental mode, the damping ratio increases with crack formation due to the energy dissipation at the crack and varies randomly for other modes. (iv) the predicted FRF curves using ANN model is highly justified with the experimental experimental FRF curves. (v) it is challenging to make valid perception about mode shapes. (vi) it is found that predicted FRF curves for all cases of cracks using ANN model have good agreement with the experimental FRF curves. This work can be extended to crack orientation detection in composite plate and shell structures using machine learning algorithm based on vibration characteristics.

Data Availability The data that support the findings of this study are available on request from the corresponding author.

Declarations

Conflict of Interest The authors state that they have no known conflicting financial or personal interests that may have seemed to affect the work presented in this study.

References

1. Özbek Ö, Doğan NF, Bozkurt ÖY (2020) An experimental investigation on lateral crushing response of glass/carbon intraply hybrid filament wound composite pipes. J Braz Soc Mech Sci Eng 42:1–13
2. Tita V, Carvalho JD, Lirani J (2003) Theoretical and experimental dynamic analysis of fiber reinforced composite beams. J Braz Soc Mech Sci Eng 25:306–310
3. Zara A, Belaidi I, Khatir S, Brahim AO, Boutchicha D, Wahab MA (2023) Damage detection in gfrp composite structures by improved artificial neural network using new optimization techniques. Compos Struct 305:116475
4. Zhang Z, Shankar K, Tahtali M, Morozov E (2010) "Vibration modelling of composite laminates with delamination damage," in proceedings of 20th International Congress on Acoustics, ICA,
5. Dewangan HC, Panda SK, Hirwani CK (2021) Numerical deflection and stress prediction of cutout borne damaged composite flat/curved panel structure. Structures 31:660–670
6. Chaupal P, Kumar D (2022) "Progressive damage analysis of random oriented chopped glass fiber-reinforced laminate under three-point bending test," Journal of The Institution of Engineers (India): Series D, pp. 1–14
7. Das MT, Yılmaz A (2018) Experimental modal analysis of curved composite beam with transverse open crack. J Sound Vib 436:155–164
8. Sahu S, Das P (2020) Experimental and numerical studies on vibration of laminated composite beam with transverse multiple cracks. Mech Syst Signal Process 135:106398
9. Jamia N, Rajendran P, El-Borgi S, Friswell M (2018) Mistuning identification in a bladed disk using wavelet packet transform. Acta Mech 229:1275–1295
10. Doebling SW, Farrar CR, Prime MB, Shevitz DW (1996) "Damage identification and health monitoring of structural and mechanical systems from changes in their vibration characteristics: a literature review," N.p,
11. Sahoo S, Jena PC (2021) Analysis of gfrp cracked cantilever beam using artificial neural network. Mater Today: Proceed 44:1788–1793
12. Chaupal P, Rajendran P (2023) A review on recent developments in vibration-based damage identification methods for laminated composite structures: 2010–2022. Compos Struct 311:116809
13. Kasinos S, Palmeri A, Lombardo M (2015) Using the vibration envelope as a damage-sensitive feature in composite beam structures. Structures 1:67–75
14. Yan Y, Cheng L, Wu Z, Yam L (2007) Development in vibration-based structural damage detection technique. Mech Syst Signal Process 21(5):2198–2211
15. Shen XJ, Lan JX, Yang XR, Ji F (2012) Modal analysis of laminated composite beams based on elastic wave theory. Appl Mech Mater 151:275–280
16. Rao SS (2019) Vibration of continuous systems. John Wiley & Sons,
17. Khalate A, Bhagwat V (2016) Detection of cracks present in composite cantilever beam by vibration analysis technique. IJISET-Int J Innov Sci, Eng Technol 3(1):400–404
18. Jena PC, Parhi DR, Pohit G (2016) Dynamic study of composite cracked beam by changing the angle of bidirectional fibres. Iran J Sci Technol, Trans A: Sci 40:27–37
19. Mehdi H, Upadhyay R, Mehra R, Singhal A (2014) Modal analysis of composite beam reinforced by aluminium-synthetic fibers with and without multiple cracks using ansys. Int J Mech Eng (IJME) 4:70–80
20. Kisa M (2004) Free vibration analysis of a cantilever composite beam with multiple cracks. Compos Sci Technol 64(9):1391–1402
21. Krawczuk M, Ostachowicz W, Zak A (1997) Modal analysis of cracked, unidirectional composite beam. Compos B Eng 28(5–6):641–650
22. Ramanamurthy E, Chandrasekaran K, Nishant G (2011) "Vibration analysis on a composite beam to identify damage and damage severity using finite element method," Int J Eng Sci Technol (IJEST), 3(7)
23. Manoach E, Warminski J, Kloda L, Teter A (2016) Vibration based methods for damage detection in structures. MATEC Web Conf 83:05007

24. Kahya V, Okur FY, Karaca S, Altunışık AC, Aslan M (2021) Multiple damage detection in laminated composite beams using automated model update. Structures 34:1665–1683
25. Dolinski L, Krawczuk M (2020) Analysis of modal parameters using a statistical approach for condition monitoring of the wind turbine blade. Appl Sci 10(17):5878
26. Gorgin R (2020) Damage identification technique based on mode shape analysis of beam structures. Structures 27:2300–2308
27. Yazdanpanaha O, Seyedpoor S (2015) A new damage detection indicator for beams based on mode shape data. Struct Eng Mech 53(4):725–744
28. Rajendran P, Srinivasan SM (2015) Performance of rotational mode based indices in identification of added mass in beams. Struct Eng Mech 54:711–723
29. Demir E (2016) A study on natural frequencies and damping ratios of composite beams with holes. Steel Compos Struct 21(6):1211–1226
30. Kıral Z, İçten BM, Kıral BG (2012) Effect of impact failure on the damping characteristics of beam-like composite structures. Compos B Eng 43(8):3053–3060
31. Kyriazoglou C, Le Page B, Guild F (2004) Vibration damping for crack detection in composite laminates. Compos A Appl Sci Manuf 35(7–8):945–953
32. Rajendran P, Srinivasan SM (2016) Identification of added mass in the composite plate structure based on wavelet packet transform. Strain 52(1):14–25
33. Rajendran P, Sivakumar SM (2015) Rotational-mode-shape-based added mass identification using wavelet packet transform. Int J Comput Methods Eng Sci Mech 16(3):182–187
34. Chaupal P, Rajendran P (2023) Flexural strength prediction of randomly oriented chopped glass fiber composite laminate using artificial neural network. J Braz Soc Mech Sci Eng 45(3):131
35. Tan ZX, Thambiratnam DP, Chan TH, Gordan M, Abdul Razak H (2020) Damage detection in steel-concrete composite bridge using vibration characteristics and artificial neural network. Struct Infrastruct Eng 16(9):1247–1261
36. Jena PC, Parhi DR, Pohit G (2019) Dynamic investigation of frp cracked beam using neural network technique. J Vib Eng Technol 7:647–661
37. Mojtahedi A, Hokmabady H, Kouhi M, Mohammadyzadeh S (2022) A novel ann-rdt approach for damage detection of a composite panel employing contact and non-contact measuring data. Compos Struct 279:114794
38. Zhang Z, Pan J, Luo W, Ramakrishnan KR, Singh HK (2019) Vibration-based delamination detection in curved composite plates. Compos A Appl Sci Manuf 119:261–274
39. Oliver GA, Ancelotti AC, Gomes GF (2021) Neural network-based damage identification in composite laminated plates using frequency shifts. Neural Comput Appl 33:3183–3194
40. Reis PA, Iwasaki KM, Voltz LR, Cardoso EL, Medeiros RD (2022) Damage detection of composite beams using vibration response and artificial neural networks. Proceed Inst Mech Eng, Part L: J Mater: Des Appl 236(7):1419–1430
41. Sreekanth T, Senthilkumar M, Reddy SM (2021) Vibration-based delamination evaluation in gfrp composite beams using ann. Polym Polym Compos 29(9):S317–S324
42. Sreekanth T, Senthilkumar M, Reddy SM (2023) Artificial neural network based delamination prediction in composite plates using vibration signals. Frat ed Integr Strutt 17(63):37–45
43. Srinivasa C, Bharath K (2011) Impact and hardness properties of areca fiber-epoxy reinforced composites. J Mater Environ Sci 2(4):351–356
44. Shin P-S, Wang Z-J, Kwon D-J, Choi J-Y, Sung I, Jin D-S, Kang S-W, Kim J-C, DeVries KL, Park J-M (2015) Optimum mixing ratio of epoxy for glass fiber reinforced composites with high thermal stability. Compos B Eng 79:132–137
45. Albu F, Mateescu A, Dumitriu N (1997) "Architecture selection for a multilayer feedforward network," in International conference on microelectronics and computer science, 131–134, Citeseer,